

Stability of organic carbon in deep soil layers controlled by fresh carbon supply

Sébastien Fontaine¹, Sébastien Barot², Pierre Barré³, Nadia Bdioui¹, Bruno Mary⁴ & Cornelia Rumpel³

The world's soils store more carbon than is present in biomass and in the atmosphere¹. Little is known, however, about the factors controlling the stability of soil organic carbon stocks^{2–4} and the response of the soil carbon pool to climate change remains uncertain^{5,6}. We investigated the stability of carbon in deep soil layers in one soil profile by combining physical and chemical characterization of organic carbon, soil incubations and radiocarbon dating. Here we show that the supply of fresh plant-derived carbon to the subsoil (0.6–0.8 m depth) stimulated the microbial mineralization of $2,567 \pm 226$ -year-old carbon. Our results support the previously suggested idea⁷ that in the absence of fresh organic carbon, an essential source of energy for soil microbes, the stability of organic carbon in deep soil layers is maintained. We propose that a lack of supply of fresh carbon may prevent the decomposition of the organic carbon pool in deep soil layers in response to future changes in temperature. Any change in land use and agricultural practice that increases the distribution of fresh carbon along the soil profile^{1,8,9} could however stimulate the loss of ancient buried carbon.

The soil reservoir of organic carbon corresponds to 615 Gt C in the top 0.2 m layer and 2,344 Gt C at depths of up to 3 m, which is more than biomass and atmospheric CO₂ combined¹. The mean residence time (MRT) of soil organic carbon (SOC) increases strongly with depth, reaching values of 2,000–10,000 yr in deep soil layers (>0.2 m)^{2–4}. However, little is known about the factors controlling the stability of carbon in deep soil layers. Improved knowledge of these factors is essential to determine whether this pool of carbon will react to global change and accelerate the increase in atmospheric CO₂.

We investigated the stability of carbon in deep soil layers in a soil profile located within the research observatory on grasslands set up by the French National Institute for Agricultural Research in 2003 (Massif Central, France). This site has been under grassland for >50 yr, and was covered with forests of chestnut and hornbeam 2,000 yr ago¹⁰. Radiocarbon (¹⁴C) dating suggests that SOC stored in deep layers is derived from these old forests (Table 1). SOC content declines with depth, but $77 \pm 1\%$ (mean \pm s.e.m.) of the soil reservoir of carbon is below 0.2 m (Supplementary Table 1). The soil is a drained Cambisol developed from granitic rock. Cambisols, which are relatively rich in deep C and cover 10% of the terrestrial surface, are the second most widespread soil type of the world after Leptosols, which are poor in deep C¹¹.

It has been widely demonstrated that the chemical nature of organic compounds may control the intensity of decomposer activities and rates of degradation. To test whether the stability of deep C is due to its inherent chemical structure, soil samples from the surface layer (0–0.2 m) and a deeper layer (0.6–0.8 m) were collected. ¹⁴C content was measured to date SOC and determine its MRT using a model of flux (Methods). The chemical composition of SOC in the

two layers was analysed by ¹³C CPMAS (cross polarization with magic-angle spinning) NMR (nuclear magnetic resonance) and by FTIR (Fourier transform infrared) spectroscopy to determine whether changes in MRT with depth may result from a shift in the chemical composition of SOC.

The ¹⁴C content of SOC declined with depth, from $100.2 \pm 0.4\%$ of modern carbon (MC%) in the surface layer to 77.9 ± 0.3 MC% in the subsoil. The ¹⁴C dating and the calculation of MRT of SOC both gave consistent results (Table 1). The surface layer was dominated by young fast-cycling carbon (320 ± 27 yr) whereas the subsoil was dominated by ancient slow-cycling carbon ($2,560 \pm 74$ yr), often referred to as the passive fraction of SOC¹². This result indicates that the decomposition of SOC is strongly reduced at depth.

These differences in MRT were not mirrored by changes in the chemical composition of SOC. Figure 1 shows that the ¹³C CPMAS NMR spectra of both layers were similar. They were characterized by dominant signals in the O-alkyl C region, which are generally assigned to amide C of proteins and to C2, C3, C5 of polysaccharides¹³. The resonance centred in the alkyl C region indicated the

Table 1 | Properties of the two soil layers

Property	Layer depth 0–0.2 m	Layer depth 0.6–0.8 m
pH	6.1 ± 0.1	6.7 ± 0
Clay (%)	27 ± 1	34 ± 1
Clay minerals*	70 ± 2	65 ± 1
Kaolinite	25 ± 1	26 ± 2
HIV	5 ± 1	9 ± 1
Illite		
Oxides	27 ± 0.1	36 ± 0.1
Fe (g kg ⁻¹)	6.5 ± 0.2	7.6 ± 0.0
Al (g kg ⁻¹)		
SOC content (g C kg ⁻¹)	32 ± 1	23.3 ± 0.5
SOC bound to minerals (% of total)	50 ± 0.5	58 ± 1
SOC $\delta^{13}\text{C}$ (‰)	-27.4 ± 0.4	-25.9 ± 0.4
SOC ¹⁴ C content (MC%)	100.2 ± 0.4	77.9 ± 0.3
SOC ¹⁴ C-age (yr BP)	Modern	$2,007 \pm 31$
SOC MRT (yr)	320 ± 27	$2,560 \pm 74$
Root (g C kg ⁻¹)	3.9 ± 0.5	0.008 ± 0.002
Root production of fresh litter† (g C kg ⁻¹ yr ⁻¹)	4.3 ± 0.6	0.009 ± 0.002
POM content (>200 µm; g C kg ⁻¹)	1.8 ± 0.7	0.016 ± 0.05
POM ¹⁴ C content (MC%)	ND	109 ± 2.8
POM MRT (yr)	ND	$6.4 \pm 4.1\ddagger$
Microbial biomass (mg C kg ⁻¹)	853 ± 11	193 ± 22

Soil properties, clay mineralogy, iron (Fe) and aluminium (Al) oxides, ¹⁴C content, ¹⁴C age and mean residence time (MRT) of soil organic carbon (SOC) and particulate organic matter (POM). Values are given as mean \pm s.e.m. ($n = 3$ for all analyses except ¹⁴C analysis of SOC and POM, $n = 2$). MC%, percentage of modern carbon; HIV, hydroxy-interlayer vermiculite; ND, not determined.

* Relative peak area of diffractograms in %.

† Root production of fresh litter was calculated as (root density)/(root MRT). Root MRT (0.9 yr) was calculated for the same grassland exposed to ¹³C labelled CO₂ (ref. 28).

‡ The model yielded two possible MRT, 6.4 ± 4.1 yr and 101 ± 35 yr, but the latter was excluded as it was inconsistent with the MRT calculated as (POM content)/(POM input flux) (Supplementary Data 2).

¹INRA, UR 874 Agronomie, 234 Avenue du Brézet, 63100 Clermont-Ferrand, France. ²IRD, UMR 137, 32 Avenue H. Varagnat, 93143 Bondy, France. ³BIOEMCO, UMR 7618, CNRS-INRA-ENS-Paris 6, Bâtiment EGER, Aile B, 78820 Thiverval-Grignon, France. ⁴INRA, UR 1158 Agronomie, Rue Fernand Christ, 02007 Laon, France.

presence of methyl C in long chain aliphatic compounds, derived from lipids¹³. Both soil layers showed signals in the aromatic region of the spectra (C substituted aryl C, and O substituted aryl C), indicative of C derived from lignin and charcoal. The only significant difference, but not quantitatively important, was a higher contribution of C substituted aryl C in the subsoil ($10 \pm 0.0\%$) than in the soil surface ($8.7 \pm 0.4\%$) ($P < 0.02$, Supplementary Table 2). The FTIR spectra also indicated that the SOC chemical composition does not change markedly with depth (Supplementary Data 1), suggesting that the stability of SOC in the subsoil is not due to the chemical structure of SOC itself.

The deep carbon may persist because it is bound to soil minerals and exists in forms that decomposers cannot access^{14,15}. Table 1 shows that the proportion of SOC bound to minerals increased slightly with depth, from $50 \pm 0.5\%$ for the surface layer to $58 \pm 1\%$ for the subsoil. Could this 8% change explain the shift in MRT of SOC with depth? We used a simple model (Supplementary Method 1) to show that the only way to simulate the shift in MRT of SOC with depth is to assume a large change in the type of organo-mineral associations, that is, organo-mineral complexes at depth must be ten times more stable than in the surface. This assumption is not supported by our results. Table 1 shows that clay mineralogy, which was dominated by kaolinite, did not change markedly with depth. Fe and Al oxides and oxyhydroxides, which play a role in the preservation of SOC, increased with depth (Fe $\times 1.3$, Al $\times 1.2$), but not to the extent imposed by our model ($\times 10$). Thus, the stability of SOC in the subsoil cannot entirely be ascribed to SOC fixation on minerals.

The slow SOC decomposition at depth could result from inappropriate conditions for microbes, such as a lack of oxygen. To test whether the overall conditions found at depth allow microbial activities, we determined MRT of particulate organic matter (POM > 200 μm). If microbial activities are possible, the small pool of root litter should be quickly recycled and dominated by recent C. This was confirmed by the results, as the MRT of POM in the deep layer was 6.4 ± 4.1 yr, in sharp contrast with SOC (Table 1).

Under these circumstances, how can deep SOC escape from microbial degradation? A new theory of SOC dynamics⁷ has proposed that the slow SOC turnover at depth results from scarcity of fresh C (plant litter and exudates). Based on many empirical results^{16–20}, this theory assumes that soil humus is the result of the

long-term accumulation of biochemically recalcitrant compounds having low energy content. Near the soil surface, microbes are able to decompose these compounds with their enzymes because they use fresh C as source of energy. In deep soil layers, however, fresh-C inputs by plants are extremely low (for example, fresh-litter deposition by roots was 478 times lower in our subsoil than in the surface layer; Table 1). Under these conditions, the theory predicts that acquisition of energy from recalcitrant compounds cannot sustain microbial activity, and soil decomposition is strongly reduced. This prediction can be experimentally tested: if the theory is right, then the delivery of fresh C to the subsoil should activate mineralization of ancient C.

To test this theory, we incubated soil sampled from the deep layer (0.6–0.8 m) with cellulose, which is the main component of plant litter. We used a novel technique based on dual labelling of cellulose (¹³C, ¹⁴C) in order to trace decomposition of cellulose C and SOC, and to determine the mean age of SOC mineralized by microbes (Methods). Soil without cellulose was also incubated as a control.

Incubation of control soil released CO₂ (Fig. 2a), indicating that there were metabolically active microbes in the subsoil and that a fraction of deep C was degraded. The ¹⁴C dating of CO₂ produced during the incubation showed that microbes in the control soils mostly decomposed recent organic matter (Table 2). Nevertheless, it is likely that decomposers mineralized a small amount of old C together with recent plant litter because the ¹⁴C content of respired CO₂ was lower than that of actual atmospheric CO₂ (~ 105 MC%).

The addition of cellulose stimulated microbial respiration and growth, demonstrating that microbes were limited by energy

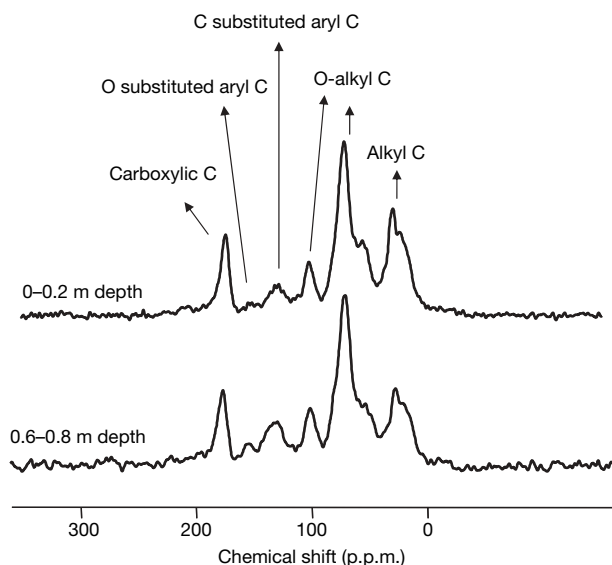


Figure 1 | ¹³C CPMAS NMR spectra of soil carbon for the two soil layers. The chemical shift regions 0–45 p.p.m., 45–110 p.p.m., 110–140 p.p.m., 140–160 p.p.m. and 160–220 p.p.m. were referred to respectively as alkyl C, O-alkyl C, C substituted aryl C, O substituted aryl C and carboxylic C.

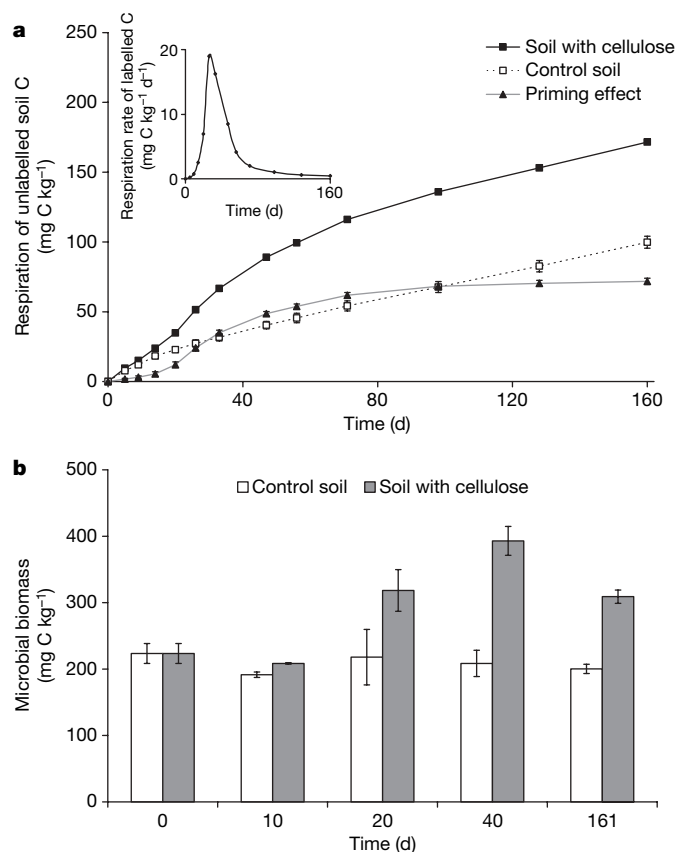


Figure 2 | Effect of cellulose supply on respiration and biomass of microbes of the deep layer. **a**, **b**, Cumulative respiration of unlabelled soil carbon (**a**) and total microbial biomass (**b**). The difference in soil carbon respiration between control and cellulose-amended soil represents the priming effect. Inset, respiration rate of labelled cellulose. The decrease in respiration after day 26 indicates the exhaustion of cellulose. Values are given as mean \pm s.e.m. ($n = 3$).

Table 2 | Properties of unlabelled soil C released during incubation

	Quantity (mg C kg ⁻¹)	¹⁴ C activity (MC%)	¹⁴ C age (yr BP)
Control soil	100 ± 4	97 ± 1.4	222 (+119/–117)
Soil with cellulose	172 ± 3	85 ± 1.6	1,329 (+154/–152)
Priming effect	72 ± 2	73 ± 2	2,567 (+226/–219)

Quantity, ¹⁴C activity and ¹⁴C age of unlabelled soil C released as CO₂ by the control, the soil with cellulose and the priming effect during the 161 days of incubation of the subsoil. Values are given as mean ± s.e.m. (n = 3). Standard errors of ¹⁴C age are asymmetric owing to the exponential decay of ¹⁴C.

(Fig. 2). The stimulation of decomposers induced a significant ($P < 0.001$, analysis of variance, ANOVA) increase in production of unlabelled soil-originated CO₂, an effect known as priming^{16–20}. It has been previously proposed that the priming effect may result from decomposition of recalcitrant old SOC by stimulated microbes. However, this hypothesis has not been demonstrated^{7,16}. Here, we show that the ¹⁴C content of the CO₂ derived from SOC decreased significantly ($P < 0.01$, ANOVA) after cellulose supply, demonstrating that cellulose-stimulated decomposers degraded very old C (Table 2). Calculations indicated that the pool of carbon decomposed by the priming effect was $2,567 \pm 226$ yr old.

Both the total microbial biomass and the priming effect significantly decreased ($P < 0.01$, ANOVA) with the exhaustion of cellulose (Fig. 2). Thus, although decomposers are able to decompose ancient C, the acquisition of energy from such substrate is not sufficient to sustain long-term biological activity. Mechanistically, this suggests that the energy required to break down the recalcitrant SOC (for example, extracellular enzyme production) is higher than the energy supplied by the catabolism of such substrate. As a result, the long-term activity of decomposer populations depends on a permanent supply of fresh C (ref. 7).

The addition of cellulose, at a rate representing about one-quarter of the annual fresh litter C deposition into the surface layer by plant roots (Table 1), led to the mineralization of 72 ± 2 mg C per kg soil of old SOC (Table 2). If this cellulose supply and the resulting priming effect were repeated each year, we calculated that, under laboratory conditions, the MRT of SOC in the subsoil would be $23,300/72 = 324$ yr, which is very close to the MRT found in the surface layer (Table 1).

The present results show that the stability of SOC in the studied deep layer reflects a lack of fresh C for microbes. We cannot be certain that the limitation by fresh C detected here, with this deep soil, will also be the dominant control of SOC stability in other deep soils. We therefore encourage research in other soils to quantify the relative role of mechanisms studied here at global scale. However, given that the breakdown of SOC is limited by the availability of fresh C in most soils^{16–20}, and that the low fresh-C availability at depth relies on a fundamental property of ecosystems (plants live and incorporate most of their litter at the surface), our results can probably be generalized to many well-drained deep soils. They cannot apply to waterlogged peat soils, because decomposition there is primarily constrained by a lack of oxygen.

Our results have several implications. First, they suggest that biological and physical processes that bury recalcitrant SOC below the deposits of fresh C protect it from decomposition and allow C storage over millennia (Supplementary Fig. 1). This mechanism provides an interesting alternative to current approaches that involve short-term storage of carbon in vulnerable compartments (plant biomass, surface SOC)²¹. Second, our incubation results suggest that, even under favourable conditions of temperature and moisture for microbial activities, SOC from the deep soil does not provide enough energy to sustain active microbial populations and thereby the production of enzymes. The existence of this energetic barrier could reduce or cancel the effect of future changes in temperature on the decomposition of this large pool of deep C, in contradiction to the predicted effect based on the temperature-induced acceleration of enzymatic reactions²². Last, our results show that deep SOC decomposition may

be reactivated. Changes in land use and agricultural practices (for example, deep ploughing versus conservation tillage, use of drought-resistant crops with deep root systems) that increase the distribution of fresh C at depth^{18,9} could stimulate loss of this ancient buried carbon.

METHODS SUMMARY

Characterization of the soil profile. Three independent soil samples were collected in layers of 0.2 m down to the depth at which unweathered parent material was encountered. Organic C and bulk density were measured in each layer to determine SOC content and storage. We studied the stability of deep SOC by focusing on two contrasted layers, that is 0–0.2 m and 0.6–0.8 m. A subsample of intact soil was used for the determination of POM²³, the remainder was sieved. The sieved soil was used to determine pH, clay content, total nitrogen, microbial C (ref. 24), age and MRT of SOC, chemical and physical composition of SOC, and to conduct the incubation.

Soil analyses. ¹⁴C content of SOC and POM (>200 µm) was measured by liquid scintillation counting. The ¹⁴C age was calculated with the Libby half-life. To determine the MRT of SOC and POM, we used the measured ¹⁴C content to constrain a flux model²⁵. The chemical composition of SOC was then analysed by CPMAS NMR ¹³C and by FTIR spectroscopy (Supplementary Data 1). The amount of C bound to soil minerals was estimated by the demineralization technique²⁶. Clay mineralogy was determined by X-ray diffraction of oriented samples. Iron and aluminium oxides and oxyhydroxides were estimated by the dithionite-citrate-bicarbonate method²⁷.

Incubation experiment. Fresh sieved soils were incubated at 20 °C and at a water potential of –100 kPa for 161 days. Dual-labelled cellulose ($\delta^{13}\text{C} = 1,860\text{‰}$, ¹⁴C activity = 2 MC%) was mixed with half of the incubated soils, 1 g cellulose C per kg of soil. The other half without cellulose (control soils) was also mixed to apply the same disturbance. The CO₂ evolved was trapped in NaOH and measured by continuous flow colorimetry. ¹³C and ¹⁴C content of CO₂ was analysed after precipitating the carbonates with excess BaCl₂. ¹³C and ¹⁴C analysis of carbonates was carried out by IRMS (isotope ratio mass spectrometry) and AMS (accelerator mass spectrometry), respectively.

Full Methods and any associated references are available in the online version of the paper at www.nature.com/nature.

Received 5 February; accepted 13 September 2007.

1. Jobbágy, E. G. & Jackson, R. B. The vertical distribution of soil organic carbon and its relation to climate and vegetation. *Ecol. Appl.* **10**, 423–436 (2000).
2. Martel, Y. A. & Paul, E. A. The use of radiocarbon dating of organic matter in the study of soil genesis. *Soil Sci. Soc. Am. Proc.* **38**, 501–506 (1974).
3. Rumpel, C., Kögel-Knabner, I. & Bruhn, F. Vertical distribution, age, and chemical composition of organic carbon in two forest soils of different pedogenesis. *Org. Geochem.* **33**, 1131–1142 (2002).
4. Schöning, I. & Kögel-Knabner, I. Chemical composition of young and old carbon pools throughout Cambisol and Luvisol profiles under forests. *Soil Biol. Biochem.* **38**, 2411–2424 (2006).
5. Luo, Y., Wan, S., Hui, D. & Wallace, L. L. Acclimatization of soil respiration to warming in a tall grass prairie. *Nature* **413**, 622–624 (2001).
6. Bellamy, P. H., Loveland, P. J., Bradley, R. I., Lark, R. M. & Kirk, G. J. D. Carbon losses from all soils across England and Wales 1978–2003. *Nature* **437**, 245–247 (2005).
7. Fontaine, S. & Barot, S. Size and functional diversity of microbe populations control plant persistence and long-term soil carbon accumulation. *Ecol. Lett.* **7**, 1075–1087 (2005).
8. Hurd, E. A. Phenotype and drought tolerance in wheat. *Agric. Meteorol.* **14**, 39–55 (1974).
9. Lal, R. Soil carbon sequestration impacts on global climate change and food security. *Science* **304**, 1623–1627 (2004).
10. Boivin, P. et al. *Volcanologie de la Chaîne des Puys* (Parc naturel régional de la chaîne des Puys, Clermont Ferrand, 2004).
11. FAO-Unesco. *Soil Map of the World (1:5,000 000)* (Unesco, Paris, 1974).
12. Jenkinson, D. S., Harkness, D. D., Vance, E. D., Adams, D. E. & Harrison, A. F. Calculating net primary production and annual input of organic matter to soil from the amount and radiocarbon content of soil organic matter. *Soil Biol. Biochem.* **24**, 295–308 (1992).
13. Kögel-Knabner, I. ¹³C and ¹⁵N NMR spectroscopy as a tool in soil organic matter studies. *Geoderma* **80**, 243–270 (1997).
14. Baldock, J. A. & Skjemstad, J. O. Role of the matrix and minerals in protecting natural organic materials against biological attack. *Org. Geochem.* **31**, 697–710 (2000).
15. Wattel-Koekkoek, E. J. W., Buurman, P., van der Plicht, J., Wattel, E. & van Breemen, N. Mean residence time of soil organic matter associated with kaolinite and smectite. *Eur. J. Soil Sci.* **54**, 269–278 (2003).
16. Kuzyakov, Y., Friedel, J. K. & Stahr, K. Review of mechanisms and quantification of priming effects. *Soil Biol. Biochem.* **32**, 1485–1498 (2000).

17. Cheng, W., Johnson, D. W. & Fu, S. Rhizosphere effects on decomposition: Controls of plant species, phenology, and fertilisation. *Soil Sci. Soc. Am. J.* **67**, 1418–1427 (2003).
18. Fontaine, S., Bardoux, G., Abbadie, L. & Mariotti, A. Carbon input to soil may decrease soil carbon content. *Ecol. Lett.* **7**, 314–320 (2004).
19. Malosso, E., English, L., Hopkins, D. W. & O'Donnell, A. G. Use of ^{13}C -labelled plant materials and ergosterol, PLFA and NLFA analyses to investigate organic matter decomposition in Antarctic soil. *Soil Biol. Biochem.* **36**, 165–175 (2003).
20. Carney, K. M., Hungate, B. A., Drake, B. G. & Megonigal, J. P. Altered soil microbial community at elevated CO_2 leads to loss of soil carbon. *Proc. Natl Acad. Sci. USA* **104**, 4990–4995 (2007).
21. Ciais, P. *et al.* Europe-wide reduction in primary productivity caused by the heat and drought in 2003. *Nature* **437**, 529–533 (2005).
22. Davidson, E. A. & Janssens, I. A. Temperature sensitivity of soil carbon decomposition and feedbacks to climate change. *Nature* **440**, 165–173 (2006).
23. Loiseau, P. & Soussana, J. F. Elevated $[\text{CO}_2]$, temperature increase and N supply effects on the turnover of below-ground carbon in a temperate grassland ecosystem. *Plant Soil* **210**, 233–247 (1999).
24. Vance, E. D., Brookes, P. C. & Jenkinson, D. S. An extraction method for measuring soil microbial biomass C. *Soil Biol. Biochem.* **19**, 703–707 (1987).
25. Hsieh, Y.-P. Radiocarbon signatures of turnover rates in active soil organic carbon pools. *Soil Sci. Soc. Am. J.* **57**, 1020–1022 (1993).
26. Eusterhues, K., Rumpel, C., Kleber, M. & Kögel-Knabner, I. Stabilisation of soil organic matter by interactions with minerals as revealed by mineral dissolution and oxidative degradation. *Org. Geochem.* **34**, 591–1600 (2003).
27. Mehra, O. P. & Jackson, M. L. Iron oxide removal from soils and clays by dithionite-citrate system buffered with sodium bicarbonate. *Clays Clay Miner.* **32**, 557–563 (1960).
28. Klumpp, K., Soussana, J. F. & Falcimagne, R. Effects of past and current disturbance on carbon cycling in grassland mesocosms. *Agric. Ecosyst. Environ.* **121**, 59–73 (2007).

Supplementary Information is linked to the online version of the paper at www.nature.com/nature.

Acknowledgements We thank S. Révaillot, J. Messaoud, S. Millon, G. Alavoine and O. Delfosse for assistance during the incubation and for chemical and isotopic analysis. We thank J.-F. Soussana, J. Bloor, R. Hakkenberg, P. Loiseau, V. Maire, A. Chabbi and K. Klumpp for critical comments on the manuscript. The Lehrstuhl für Bodenkunde, TU München, is acknowledged for providing the NMR spectrometer. The Hydrasa Laboratory (University of Poitiers) is acknowledged for providing the X-ray diffractometer. This work was financially supported by the INRA Ecology Department, the MED (GESSOL) and the ANR (BIOMOS and C Profond).

Author Contributions S.F. conceived and designed this study; C.R. performed NMR and FTIR analyses; P.B. performed clay mineralogy analyses; B.M. performed ^{13}C analyses; N.B. and S.F. jointly conducted the incubation; S.F. wrote the manuscript; S.B. commented on the manuscript, the modelling and the statistical analyses; and all authors took part in the interpretation of the results.

Author Information Reprints and permissions information is available at www.nature.com/reprints. Correspondence and requests for materials should be addressed to S.F. (fontaine@clermont.inra.fr).

METHODS

Characterization of the soil profile. Three soil samples were collected at a distance of 1–2 m from each other, and in layers of 0.2 m down to the depth at which unweathered parent material was encountered (1 m) (Supplementary Fig. 1). Each replicate was analysed separately. Organic C and bulk density were measured for each horizon to determine SOC content and storage at each depth. We studied the deep SOC stability by focusing on two contrasted layers, that is, 0–0.2 m and 0.6–0.8 m. A subsample of intact soil was used for the determination of POM²³, the remainder was sieved (2 mm) and visible plant residues were removed (sieved soil). After this treatment, POM (>200 µm), soluble C and microbial C accounted for less than 4.5% of total C in both soil layers, indicating that the remaining C is dominated by humified SOC. The sieved soil was used to determine pH, clay content, total nitrogen, microbial C²⁴, age and MRT of SOC, chemical and physical composition of SOC, and to conduct the incubation experiment. All the analyses were made in three replicates per soil layer except ¹⁴C analysis of SOC and POM that were made in two replicates per soil layer.

Chemical characterization of soil carbon. Soils were treated with 10% HF to concentrate organic C and to remove paramagnetic compounds²⁹. Solid-state ¹³C NMR spectra were obtained on a Bruker DSX-200 NMR spectrometer. CPMAS was applied at 6.8 kHz. Solid-state ¹³C NMR signal was recorded as free induction decay and Fourier-transformed to yield a NMR spectrum.

¹⁴C dating and estimation of the mean residence time of soil carbon. Soils were treated with dilute HCl before ¹⁴C measurements to remove eventual traces of carbonates. ¹⁴C content of SOC and POM, measured by liquid scintillation counting at the Centre de Datation par le Radiocarbène (France), is expressed in percentage of modern carbon (MC%), which is the percentage deviation from ¹⁴C/¹²C ratio of oxalic acid in 1950³⁰. Fast cycling C (turnover time, years–centuries) has value >100 MC% because it has incorporated a significant proportion of ¹⁴C emitted by nuclear bomb testing. Before weapons testing, atmospheric ¹⁴C was approximately 100 MC%. Slow-cycling C (turnover time, millennia) has value <100 MC% because of radioactive decay of ¹⁴C. The ¹⁴C age was calculated with the Libby half-life (5,568 yr) and expressed in years before present (yr BP). To determine the MRT of SOC and POM, we used the measured ¹⁴C content to constrain a flux model²⁵. The ¹⁴C content of SOC was modelled as:

$$A_{\text{SOC}}^{14}(t) = \frac{\sum_{i=b}^p [M_i e^{-(p-i)/\text{MRT}} \times A_i^{14} e^{-(p-i)\lambda}]}{\sum_{i=b}^p M_i e^{-(p-i)/\text{MRT}}}$$

where M_i is the amount of new SOC input to the soil in year i , MRT the mean residence time of SOC, p the year when the soil sample is taken, b the year when the simulation starts, A_i^{14} the ¹⁴C activity in the atmosphere of year i and λ the ¹⁴C decay rate (1/8,268). See Supplementary Method 2 for more details.

Carbon bound to soil minerals. Soils were treated with 10% HF to remove mineral material and release mineral-associated carbon. The carbon lost upon the demineralization procedure is assumed to represent the carbon bound to soil minerals²⁶.

Clay mineralogy, content of iron and aluminium oxides. Clay mineralogy was determined by X-ray diffraction (XRD) of oriented samples. The diffractograms, shown in Supplementary Fig. 2, were obtained with a Phillips diffractometer using Cu radiation. Peak areas of the clay minerals were measured and reported in percentages of total peak area to compare the (semiquantitative) XRD diffractograms. Iron and aluminium oxides and oxyhydroxides were estimated by the dithionite-citrate-bicarbonate method²⁷.

Incubation experiment. Experimental units consisted of 60 g (oven-dried basis) samples of fresh sieved soils placed in 500 ml flasks and incubated at 20 °C for 161 days. The moisture content of the soil was adjusted to a water potential of –100 kPa with a nutrient solution (NH₄NO₃, KH₂PO₄). After 15 days of pre-incubation, 1 g cellulose C per kg soil of dual-labelled cellulose (¹³C = 1,860‰, ¹⁴C activity = 2 MC%) was mixed with half of the incubated soils. The other half without cellulose (control soils) was also mixed to apply the same disturbance. The CO₂ evolved was trapped in NaOH and was measured by continuous flow colorimetry. ¹³C-CO₂ was analysed by an elemental analyser coupled to a mass spectrometer after precipitating the carbonates with excess BaCl₂ and filtration. Microbial C and ¹³C were determined by the fumigation-extraction technique²⁴. Measurements of ¹⁴C-CO₂ were conducted on a separate set of flasks. In this set, the NaOH solutions taken at each sampling date were kept under free CO₂ atmosphere until the end of incubation. These samples were then pooled together to produce a single sample which received BaCl₂. ¹⁴C analysis of carbonates and cellulose was carried out by AMS (Radiocarbon Laboratory of Poznań, Poland).

Calculations. The ¹⁴C content of CO₂ emitted in the control soil was transformed into age BP using the Libby half-life of ¹⁴C. Measurement of the ¹⁴C content of total CO₂ emitted in soils with cellulose does not allow for the calculation of the age of SOC released as CO₂ because of the two sources of carbon (cellulose, SOC). We circumvented this problem using dual labelling of cellulose. The ¹³C labelling of cellulose allowed the separation of soil C (R_S) and cellulose (R_C) respiration (mg C CO₂ per kg soil) using mass balance equations:

$$R_S A_S + R_C A_C = R_T A_T$$

$$R_S + R_C = R_T$$

where A_S is the ¹³C abundance (dimensionless) of soil carbon, A_C the ¹³C abundance of cellulose, R_T the total CO₂ emitted by soil with cellulose and A_T its ¹³C abundance.

Then, we calculated the ¹⁴C content (expressed in MC%) of SOC released as CO₂ (A_S^{14}) with the equation

$$R_S A_S^{14} + R_C A_C^{14} = R_T A_T^{14}$$

where A_C^{14} is the ¹⁴C content of cellulose and A_T^{14} the ¹⁴C content of the total CO₂ emitted by soil with cellulose. A_S^{14} was converted into age BP using the Libby half-life of ¹⁴C.

The priming effect (PE, mg C CO₂ per kg soil) induced by the addition of cellulose was calculated as:

$$\text{PE} = (R_S \text{ soil with cellulose}) - (R_S \text{ control soil})$$

We calculated the ¹⁴C content of the pool of SOC decomposed via the priming effect (A_{pe}^{14}) as

$$A_{\text{pe}}^{14} = \frac{(R_S \text{ soil with cellulose}) A_S^{14} - (R_S \text{ control soil}) A_{S0}^{14}}{\text{PE}}$$

where A_{S0}^{14} is the ¹⁴C content of CO₂ emitted in the control soil. A_{pe}^{14} was converted into age BP as previously described.

29. Schmidt, M. W. I., Knicker, H., Hatcher, P. G. & Kögel-Knabner, I. Improvement of ¹³C and ¹⁵N CPMAS NMR spectra of bulk soils, particle size fractions and organic material by treatment with hydrofluoric acid (10%). *Eur. J. Soil Sci.* **48**, 319–328 (1997).
30. Stuiver, M. & Polach, H. A. Discussion—reporting of ¹⁴C data. *Radiocarbon* **19**, 355–363 (1977).